Two-phase Flow Calculations in Pore Unit-cells Implementing Mixed FEM/Lattice-Boltzmann Simulators

E. D. Skouras[1,2*], A. N. Kalarakis[2], M. S. Valavanides[3], and V. N. Burganos[1]
[1]Foundation for Research and Technology, Hellas/Institute of Chemical Engineering Sciences, [2]Dept Mechanical Engineering, TEI of Western Greece, Hellas, [3]Dept Civil Engineering, Applied Mechanics Laboratory, TEI of Athens, Hellas
*Corresponding author: FORTH/ICE-HT, Stadiou str., Platani, GR-26504, Patras, Hellas, email: Eugene.Skouras@iceht.forth.gr

Abstract: Macroscopic two-phase flow in porous media is, in general, a mixture of connected and disconnected oil flow. The latter is expressed as ganglion dynamics and drop traffic flow. Disconnected flow is central in all modern simulators implementing pore network modeling. The computational effort, associated with the solution of the two-phase flow problem (including the effects of bulk viscosity and interfacial capillary pressure) within conduits of varying or complicated geometry, is a critical factor in deciding on the particular numerical scheme(s) to tackle the problem.
In the present work, realistic pore-scale CFD calculations of unit-cell conductances have been performed for various flow configurations using single- and two-phase finite element methods. These calculations have been compared against less intensive computations implementing semi-analytical lubrication approximation methods. Results show that, for the given flow and geometry settings the discrepancy between the CFD and Lubrication approximation predictions is well within an acceptable range.

Keywords: two-phase flow in porous media, permeability, relative permeabilities, pore-scale modeling

1. Introduction and scope of work

Macroscopic two-phase flow in porous media is, in general, a mixture of connected and disconnected oil flow. The latter is expressed as ganglion dynamics and drop traffic flow, patterns observed experimentally in pore network models [1, 2] and real porous media [3, 4].

Disconnected flow is always taken into account in pore network simulators. The computational load of such simulators depends on the solution of the hydrodynamic problem associated with the motion of oil/water interfaces within the complicated geometry of the pores.

Depending on the pore geometry, the flow conditions and the physicochemical properties of the two phases, there are different modeling approaches to tackle the problem: lubrication approximation, finite elements, lattice-Boltzmann etc. Each approach has different pros and cons. Lubrication approximation is –in general-computationally inexpensive but it can only be implemented if appropriate analytical expressions are available for the particular type of flow geometry and flow conditions, e.g. cases when creeping flow within cylindrical geometries are considered. Finite elements methods are applicable in many complicated types of geometry as long as computational resources are available. Lattice-Boltzmann methodologies have no real problem in the geometry setting but do not comply with all types of (imposed) physicochemical properties of the fluids.

Pore network simulators may implement any one of the aforementioned methods (exclusively or in combination). They normally solve the (pore-scale) flow problem within individual unit-cells or representative elementary volumes (so called REVs -comprising ensembles of unit-cells) in terms of the locally induced flow conditions. Then, the solutions are integrated through appropriate meso-to-macro- scale consistency rules (mass /momentum /energy /other balances) into an average macroscopic solution (pressure gradient and/or superficial velocities).

1.1 The *DeProF* model

A similar modeling approach is implemented in the *DeProF* true-to-mechanism model developed by Valavanides & Payatakes [5, 6]. The model is based on the concept of decomposition of the macroscopic flow into prototype flows, hence the acronym *DeProF*. The associated algorithm computes the reduced

macroscopic pressure gradient for oil and water given the values of the imposed flowrates of oil and water, under immiscible, steady-state, two-phase flow conditions in pore networks.

The computational effectiveness of the *DeProF* algorithm, (up to ~5 mins per complete simulation on a typical desktop computer, depending on the values of system and operational parameters) is based on an inherent hierarchical theoretical modeling approach: at pore scale, the different configurations of two-phase flow within unit cells [imbibition and drainage invoking larger non-wetting blobs (ganglia and large droplets) within pores, and core annular flow of tiny non-wetting droplets within pore throats] are modeled by implementing relatively simple computational schemes, i.e. lubrication approximation of Stokes flow and Young-Laplace law for the interfacial tension, to derive the corresponding unit cell conductances. Then, the fractional distribution of conductances is scaled-up, using effective medium theory and mass & flowrate balances, into a macroscopic description of the flow.

Combining effective medium theory with appropriate expressions for pore-to-macro scale consistency for oil and water mass transport, it takes into account the pore-scale mechanisms and the network wide cooperative effects as well as the sources of non-linearity (caused by the motion of interfaces) and other complex effects.

The computational efficiency of the *DeProF* model is based on the minimum use of computational resources (CPU time) in combination to the specificity in its predictions. The basic elementary computational schemes used in the *DeProF* model algorithm implement Lubrication Approximation for the description of the conductances [6].

Extensive *DeProF* model simulations have been carried out in the past, for different unit cell geometries (2D pore networks implementing "blister-and-flat-stick" type u.c. and 3D networks implementing "ball-and-stick" type u.c.) and different wetting conditions [7].

In the present work we try to benchmark the core, pore scale modeling approach implemented in those simulations against more realistic pore-scale flow calculations (CFD). In this context we have calculated the conductances of typical unit-cells of the chamber-and-throat type, for various flow configurations (single phase, two-phase oil-water interfaces). Appropriate numerical schemes, using single- and two-phase finite element methods have been implemented within the COMSOL™ platform.

2. Methodology

2.1 Description of the flow problem

The immiscible two-phase flow problem is considered within typical chamber-and-throat type pore unit-cells comprising model pore networks. In specific, the "blister-and-flat-stick" type, identical to the unit-cells of the 2D pore network considered in [6, 7] were used. They consist of two short cylinders of classes -*j* and -*k*, linked together with a rectilinear cylindrical throat of elliptical cross section of class-*i*, see Fig.1. This type of unit-cell geometry is inherently more difficult to tackle when compared to the axisymmetric "ball-and-stick" type of unit-cells comprising the 3D network.

The network skeleton is a square lattice with node-to-node distance l = 1221 μm. For this particular network, the lattice dimensionality is N_d = 2, and the coordination number is σ = 4. The principal axis of the cylindrical throat's elliptical cross section (perpendicular to the plane of the unit-cell) represents the maximum pore depth and it is uniform set at D_T = 115 μm for all unit-cells.

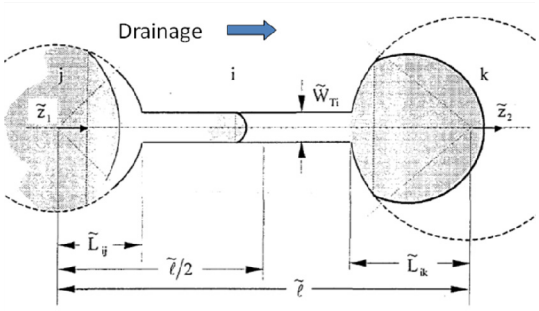

Figure 1. Schematic of the geometric unit-cell parameters [6]. Dark areas represent (ideally) different positions of the invading oil (water is drained from left to right), as applied in the lubrication approximation solution of the flow problem.

The chamber size (diameter) distribution and the throat size (width) distribution have discrete (composed of five classes each) nearly normal size distributions with mean values D_{Cj} = 610 μm, W_{Tj} = 169 μm and standard deviations equal

to 1/4 of the corresponding mean values [6]. The occurrence probabilities f_j of each class along with the respective actual characteristic dimensions of the chambers (diameters), D_{Cj}, and the throats (widths), W_{Tj}, as well as more details on the precise geometry, are described in [5-8].

Critical geometric unit-cell parameters, include the following dimensionless terms: the reduced throat-i half-width (or throat-to-chamber aspect ratio), ξ_{ji}, the equipotential lines at the end of the unit-cell, u_1, and at the chamber-throat junction (bipolar coordinate system), u_{0ij}, and the distance of the latter from the chamber center, x_{0ij},

$$\xi_{ij} = \frac{W_{Ti}}{D_{Cj}}, \quad u_1 = \cosh^{-1}\left(\sqrt{2}\right),$$

$$u_{0ij} = \cosh^{-1}\left(\frac{1}{\xi_{ij}}\right), \quad x_{0ij} = \frac{D_{Cj}}{2}\frac{\sqrt{1-\xi_{ij}^{\,2}}}{1+\xi_{ij}}$$

2.2 Lubrication Approximation

Implementing the lubrication approximation, the total pressure drop across any *jik*-class unit cell can be described as:

$$\begin{aligned}\Delta\tilde{p}_{jik} &= \Delta\tilde{p}_{jik}^{1\Phi} + \Delta\tilde{p}_{jik}^{ow} \\ &= \left(\tilde{\mu}_o\frac{\tilde{z}}{\tilde{\ell}} + \tilde{\mu}_w\frac{\tilde{\ell}-\tilde{z}}{\tilde{\ell}}\right)\frac{\tilde{q}_{uc}}{\tilde{\ell}^3}A_{jik}^{1\Phi} + 2\frac{\tilde{\gamma}_{ow}}{\tilde{\ell}}H_j^{1\Phi}\left(\tilde{z}\right)\end{aligned}$$

Coefficient $A_{jik}^{1\Phi}$ represents the effect of the particular unit-cell geometry on the contribution of the bulk phase viscosity on the total pressure drop and is given by

$$\begin{aligned}A_{jik}^{1\Phi} &= 12\frac{1}{D_T}\left(u_{0ij}+u_{0ik}-2u_1\right) \\ &+ \frac{64}{\pi}\frac{W_{Ti}^{\,2}+D_T^{\,2}}{W_{Ti}^{\,3}D_T^{\,3}}\left(1-x_{0ij}-x_{0ik}\right)\end{aligned}$$

Similarly, coefficient $H_j^{1\Phi}$ represents the effect of the particular unit-cell geometry on the contribution of the o/w interface capillary pressure (implementing Young-Laplace law)

$$\begin{aligned}H_j^{1\Phi}\left(\tilde{z};\theta\right) &= \frac{\cos\theta}{D_T} \\ &+ \frac{1}{D_{Cj}}\left(\cos\theta - \sin\theta\frac{\tilde{z}}{\sqrt{\left(\tilde{D}_{Cj}/2\right)^2-\tilde{z}^2}}\right)\end{aligned}$$

Both expressions are given in terms of the position of the o/w interface along the unit-cell, z. The unit-cell conductance is estimated by integrating the pressure drop along the unit-cell.

2.3 CFD (mixed FEM/L-B)

Two-phase flow conductances (absolute permeabilities) of *jik*-class unit cells were also estimated with transient Level-Set multiphase FEM methods with moving mesh at the interfaces [9, 10], and Lattice-Boltzmann two-phase flow simulators with the BGK approximation [11] for validation purposes in selected cases.

The following flow configurations have been considered:

(i) Single-phase water and oil flow;

(ii) Two-phase wetting/ non-wetting flow (immiscible) with the interface contacting - at fixed angle- the pore conduit walls for cases:

(ii.a) Receding interface across a *jik* unit-cell (gradual drainage)

(ii.b) Advancing interface across a *jik* unit-cell (gradual imbibition).

Conductivities were calculated for predefined values of velocities or pressure gradients to deliver appropriate look-up tables (maps). The numerically calculated values of the simple pore conductivities have been compared with the conventional approaches (lubrication approximation) already used in the basic versions of the *DeProF* algorithm.

3. Results

3.1 FEM simulations

The basic geometric configuration of a characteristic (2D) unit cell that uses all available symmetries to minimize computational burden is shown in Figures 2-7. In the physical

description, multiphase (Oil-Water) simulations using either stationary of moving mesh have been adopted for the domain discretization, and the solution was obtained using transient implicit solvers implemented in Comsol.

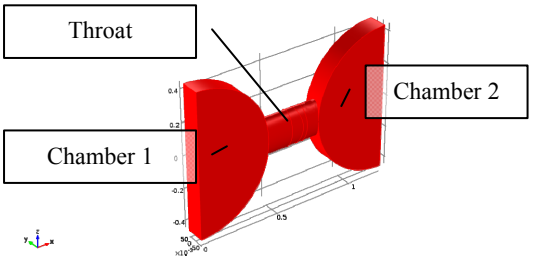

Figure 2. Full geometry view (D_{c1}=880µm, D_{c2}=880µm, W_t=222µm)

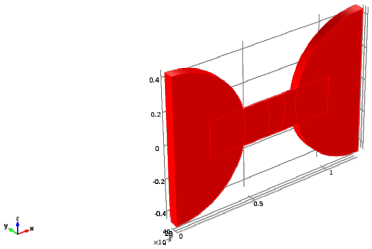

Figure 3.Half geometry view (D_{c1}=880µm, D_{c2}=880µm, W_t=222µm)

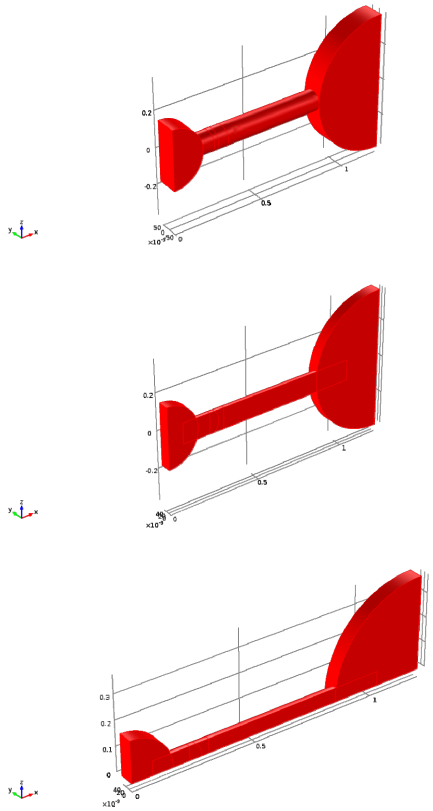

Figure 5.Full (up), half (middle) & quarter (bottom) geometry view for (D_{c1}=330µm, D_{c2}=750µm, W_t=111µm)

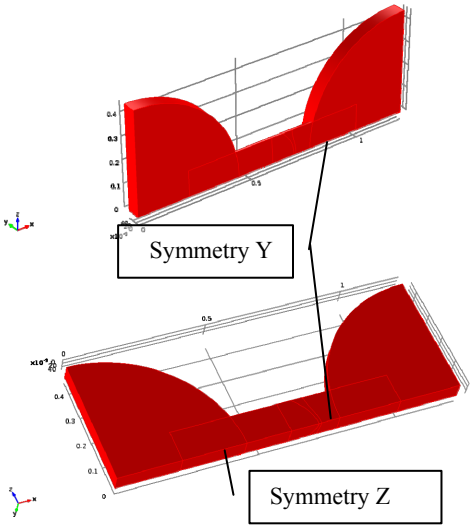

Figure 4.Quarter geometry view (D_{c1}=880µm, D_{c2}=880µm, W_t=222µm):

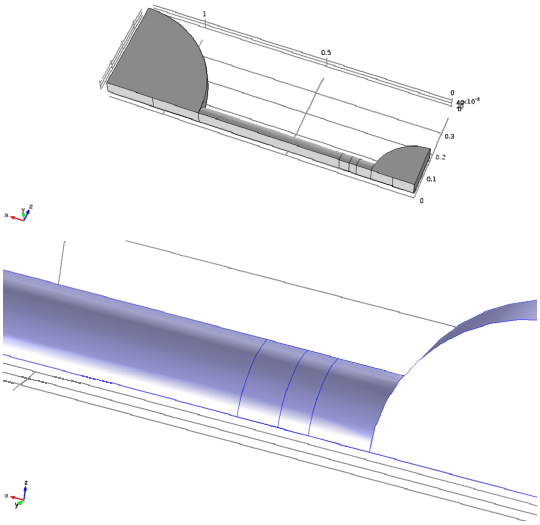

Figure 6.Quarter geometry view (D_{c1}=330µm, D_{c2}=750µm, W_t=111µm).

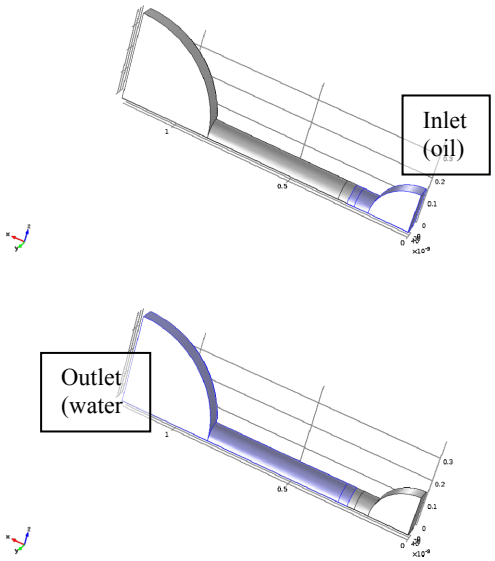

Figure 7. Quarter geometry view (D_{c1}=330µm, D_{c2}=750µm, W_t=111µm). Top: Oil (inlet) domain, bottom: Water (outlet) domain

Initially the interface is assumed flat, Figure 8. Then, it is allowed to equilibrate under only the surface tension force at specific contact angle (theta=42°) on the wall side (no flow yet), Figure 9. Then, pressure gradient is applied on both ends, Figure 10, with the outlet face (water) fixed at 0 [Pa] (averaged), while the entrance/ inlet face pressure is regulated in order to obtain a fixed velocity in the interior of the throat: *velocity* = $n\ D_t/\Delta t$, with n=5 (on small D_c,W_t) or 2.5 (on large D_c,W_t), while Δt=3s is the duration of the transient simulations.

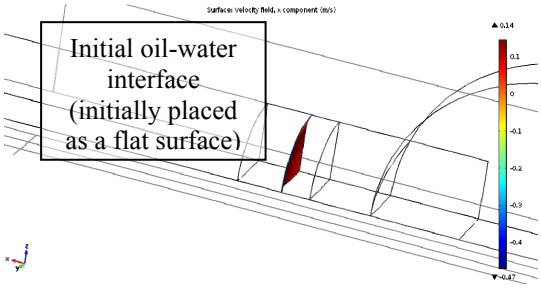

Figure 8.Quarter geometry view (D_{c1}=330µm, D_{c2}=750µm, W_t=111µm): interface after t=0 s

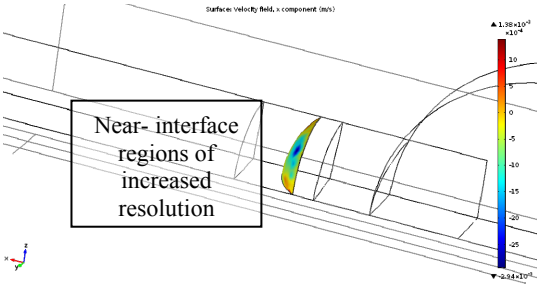

Figure 9.Quarter geometry view (D_{c1}=330µm, D_{c2}=750µm, W_t=111µm): interface at equilibrium (no pressure gradient applied)

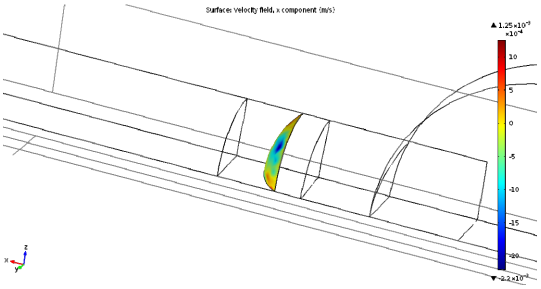

Figure 10.Quarter geometry view (D_{c1}=330µm, D_{c2}=750µm, W_t=111µm): interface 3 seconds after equilibrium (and pressure gradient applied)

Results obtained tabulated the average and maximum pressures, and the volume flux at the inlet face of each chamber-throat configuration at the end of each transient run, while detailed results at each time step are also available in case they are of interest.

Figure 11 displays relative two-phase Level-set simulations of drainage without moving mesh. Comparison of the performance of CFD (Level-set) and typical lubrication-approximation results are shown in Figure 12, where errors up to ~10% can be observed. Those values are within the expected range, given the assumptions and the simplifications used to derive the analytical solutions.

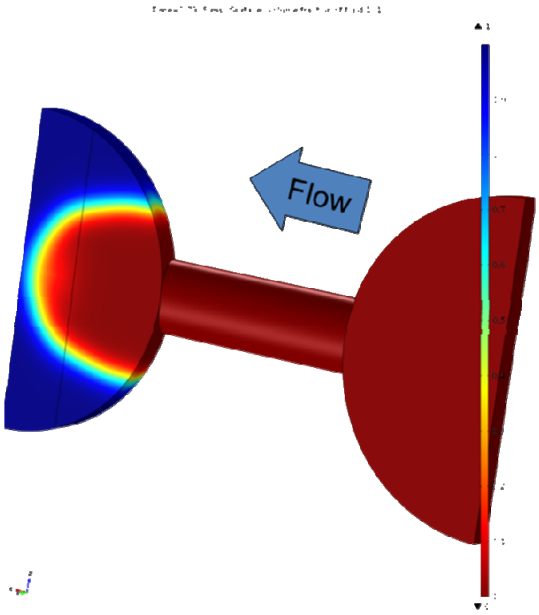

Figure 11. Full geometry view (D_{Cj}=D_{Ck}=750µm, W_t=169µm), interface in the interior of the exit chamber. Color coding depending on the volume fractions (red: 100% oil, blue:100% water)

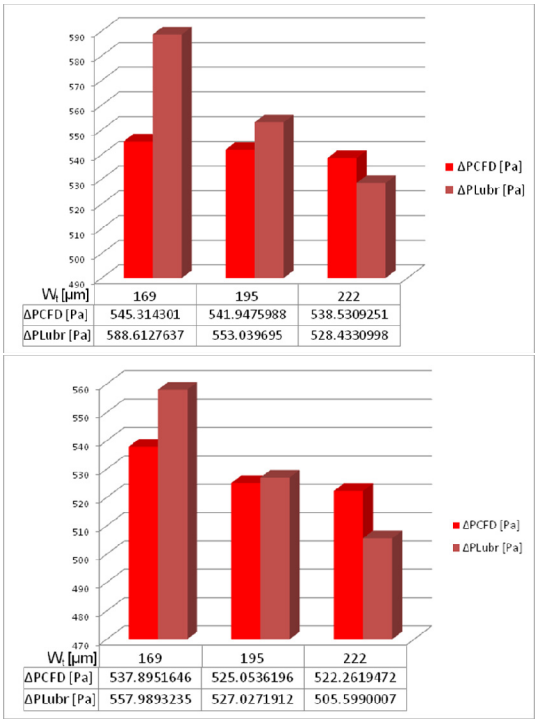

Figure 12. Comparison of the efficiency of current CFD calculations and the original ones obtained with lubrication-theory approximations. Top: $D_{Cj} = D_{Ck} =$ 750µm, bottom: $D_{Cj} =$ 750µm, $D_{Ck} =$ 890µm

5. Conclusions

The absolute permeabilities of two-phase flow in *jik*-class unit cells were calculated with sophisticated transient Level-Set multiphase FEM methods using moving mesh at the water-oil interfaces. Results were delivered for single- and two-phase water and oil flow, either wetting/non-wetting (immiscible) flow with the w/n-w interface contacting the pore conduit walls, for receding and advancing w/n-w interface across a *jik* unit-cell (gradual drainage or imbibition, respectively).

Comparison of results with analytical estimations using lubrication approximation presented errors up to ~10%, a range consistent with the level of modeling assumptions.

6. References

1. D.G. Avraam, A.C. Payatakes, Flow regimes and relative permeabilities during steady-state two-phase flow in porous media, *J. Fluid Mech.*, **293**, 207-236 (1995)

2. K.T. Tallakstad, H.A. Knudsen, T. Ramstad, G. Løvoll, K.J. Måløy, R. Toussaint, E.G. Flekkøy, Steady-State Two-Phase Flow in Porous Media: Statistics and Transport Properties, *Phys. Rev. Lett.*, **102**, 074502 (2009)

3. A. Georgiadis, S. Berg, A. Makurat, G. Maitland, H. Ott, Pore-scale micro-computed-tomography imaging: Nonwetting-phase cluster-size distribution during drainage and imbibition, *Phys. Rev. E*, **88**, 033002 (2013)

4. S. Youssef, E. Rosenberg, H. Deschamps, R. Oughanem, E. Maire, R. Mokso, Oil ganglia dynamics in natural porous media during surfactant flooding captured by ultra-fast x-ray microtomography, *Symposium of the Society of Core Analysts* (2014)

5. M.S. Valavanides, A.C. Payatakes, True-to-mechanism model of steady-state two-phase flow in porous media, using decomposition into prototype flows, *Adv. Water Resour.*, **24**, 385-407 (2001)

6. M.S. Valavanides, Steady-State Two-Phase Flow in Porous Media: Review of Progress in the Development of the DeProF Theory Bridging Pore to Statistical Thermodynamics Scales, *Oil Gas Sci. Technol. – Rev. IFP Energies nouvelles*, **67**, 787-804 (2012)

7. M.S. Valavanides, A.C. Payatakes, Effects of Pore Network Characteristics on Steady-State Two-Phase Flow Based on a True-to-Mechanism Model (DeProF) *10th ADIPEC Abu Dhabi International Petroleum Exhibition & Conference*, 379-387 (2002)
8. ibid., Wetting film effects on steady-state two-phase flow in pore networks using the DeProF theoretical model, *11th ADIPEC: Abu Dhabi International Petroleum Exhibition and Conference*, 517-526 (2004)
9. E. Olsson, G. Kreiss, A conservative level set method for two phase flow, *J. Comput. Phys.*, **210**, 225-246 (2005)
10. E. Olsson, G. Kreiss, S. Zahedi, A conservative level set method for two phase flow II, *J. Comput. Phys.*, **225**, 785-807 (2007)
11. A.N. Kalarakis, V.N. Burganos, A.C. Payatakes, Galilean-invariant lattice-Boltzmann simulation of liquid-vapor interface dynamics, *Phys. Rev. E Stat. Nonlinear Soft Matter Phys.*, **65**, 056702/056701-056702/056713 (2002)

7. Acknowledgements

Research partially funded by the European Union (European Social Fund-ESF) and Greek national funds through the Operational Program "Education and Lifelong Learning“, action Archimedes III, project “Archimedes III: Funding of Research Groups in TEI of Athens” (MIS 379389).